J Low Temp Phys (2011) 162: 669–677
DOI 10.1007/s10909-010-0330-0

High Quality Tuning Forks in Superfluid ^{3}He-B Below 200 μK

Marcel Človečko · Emil Gažo · Martin Kupka · Maroš Skyba · Peter Skyba

Received: 3 August 2010 / Accepted: 7 December 2010 / Published online: 22 December 2010

Abstract We have investigated the influence of the damping force acting on high quality tuning forks ($Q \sim 10^6$) of different sizes and geometries in superfluid ^{3}He-B at temperatures below 200 μK and a pressure of 0.1 bar. The measurements show that at low velocities, the damping of the largest fork expressed in terms of its resonance characteristic width Δf_2 rises up as its velocity increases. This is in contradiction to the damping of the fork due to Andreev reflection and it may be caused by the interaction of this fork with excitations trapped in the Andreev bond states. We present our preliminary experimental results.

Keywords Mechanical resonators · Tuning forks · Superfluid ^{3}He-B · Andreev reflection · Andreev bound states

1 Introduction

Recently, the tuning forks became a very popular experimental tool used in low temperature physics for various applications like thermometry in cryogenic fluids [1–3], generation and detection of quantum turbulence in superfluids and mixtures [4–8], the study of the Andreev reflection in superfluid ^{3}He-B [9–11], the "surface" microscopy in STM, AFM techniques [12], etc. Being commercially available and used mainly as a "time reference" for watches, the producers fabricate the tuning forks of various sizes and shapes with the resonance frequency $\sim 2^{15}$ Hz. This broad commercial availability offers an opportunity that the tuning forks may become and may serve as a reference standard in low temperature physics.

M. Človečko · E. Gažo · M. Kupka · M. Skyba · P. Skyba (✉)
Centre of Low Temperature Physics, Institute of Experimental Physics, SAS and P.J. Šafárik University Košice, Watsonova 47, 04001 Košice, Slovakia
e-mail: skyba@saske.sk

As the tuning forks are commercially available in various geometries and sizes, quite naturally a question arises, whether and how the different size and geometry of the tuning forks affects the mutual interaction between the fork and a fluid surrounding it. Here, in this contribution we present preliminary experimental results of our study with the aim to compare the behaviors of these mechanical resonators with different geometries (and surfaces) in superfluid ^{3}He-B in the ballistic regime at temperatures below 200 μK and a pressure of 0.1 bar.

2 Experimental Details

Using the simplest, one dimensional physical model, the fork motion in a fluid is described by the well known equation

$$\frac{d^2x}{dt^2} + \gamma \frac{dx}{dt} + \omega_0^2 x = F_0 \exp(i\omega t). \tag{1}$$

The right side is equal to the electric part of the Lorentz force $F_0 = nqE/m$ (instead of the magnetic part in case of vibrating wire) where E is the electric field intensity, n is the number of atoms with charge q. In (1) γ is the complex constant per unit of mass ($\gamma = \gamma_2 + i\gamma_1$) characterizing the resistance of the fluid against the fork motion and ω_0 is the fork resonance frequency in vacuum, usually well defined by the forks manufacturers.

In the solution to (1), the velocity v at which the fork moves through the fluid depends on the frequency and amplitude of the driving force and on the properties of the fluid (expressed by the constant γ) as

$$v(\omega) = v_0 \frac{\gamma_2^2\omega^2 + i\gamma_2\omega(\omega_0^2 - \omega^2 - \gamma_1\omega)}{(\omega_0^2 - \omega^2 - \gamma_1\omega)^2 + \gamma_2^2\omega^2}, \tag{2}$$

where v_0 is the maximum velocity amplitude at the resonance frequency ω_{R0} and depends on the driving force amplitude F_0. The resonance frequency ω_{R0} can be calculated from the expression $Im[v(\omega)] = 0$.

The tuning fork is brought into resonance by the application of an AC harmonic voltage on its electrodes. The electric field arising between these electrodes polarizes the atoms and this polarization process is associated with the crystal lattice deformation manifested in the form of the prong displacement. The magnitude of the prong displacement depends on the interaction of the fork with the surroundings (neglecting its intrinsic damping) and a balance of the corresponding forces sets the amplitude of the polarization p. Periodic changes of the electric field E produce a periodic time variation of the polarization p, that is an electric current I_F flowing through the fork. The amplitude of current I_F is proportional to the electric field E amplitude and to the rate of displacements i.e. to the velocity of the prongs $v(\omega)$

$$I_F(\omega) \approx d_{11} E v(\omega) = \alpha v(\omega), \tag{3}$$

where d_{11} is the relevant component of the piezoelectric modulus tensor, α is the proportionality constant which needs to be determined experimentally and $v(\omega)$ is

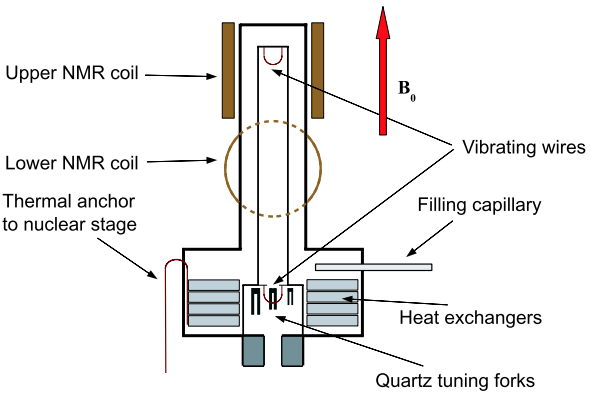

Fig. 1 (Color online) A schematic sketch of the double walled experimental cell mounted on our nuclear stage. The orientation of the magnetic field B_0 is shown as well

given by expression (2). The magnitude of the driving force acting on the fork per prong is given by [2]

$$F_{TF} = \frac{\alpha V_{TF}}{2}, \tag{4}$$

where V_{TF} is the voltage applied across the tuning fork.

The experiments were carried out in a double walled experimental cell mounted on a diffusion welded copper nuclear stage [13]. A schematic sketch of the cell is illustrated in Fig. 1. While the upper tower served for NMR measurements, in the lower part of the experimental cell, three tuning forks and one NbTi vibrating wire were mounted. The wire served as a thermometer in the ballistic regime. The tuning forks were taken out from their original sealed metallic case and the former wires were replaced by copper wires. The copper wires were electrically connected to the pads of the tuning forks using tiny droplets of a silver conductive paste. After that, the wires were passed through the holes drilled in a piece of Stycast impregnated paper serving as a base and glued with Stycast epoxy resin. The base with forks was installed into the cell and the copper wires coming out from the cell were thermally connected to the nuclear stage providing thus a thermal anchor for the forks.

Each of the forks was separately excited by a harmonic voltage supplied from a programmable generator and brought into resonance by sweeping its frequency. The corresponding electric current flowing through the fork was measured using the measurement technique based on current detection by a proper current to voltage converter in combination with the lock-in techniques as described in [14]. Under this condition the voltage across the tuning fork V_{TF} is equal to the excitation voltage (assuming the negligible resistance of the electrical leads).

After cooling the fridge down to ∼0.9 K, the physical characteristics of the tuning forks in vacuum were measured in order to determine the α constants for the individual forks. All forks behaved as high Q resonators having Q value higher than 10^6. The values of α constants for all forks were determined in the way as described in [2]

$$\alpha = \sqrt{\frac{4\pi m \Delta f_2^i}{R}}, \tag{5}$$

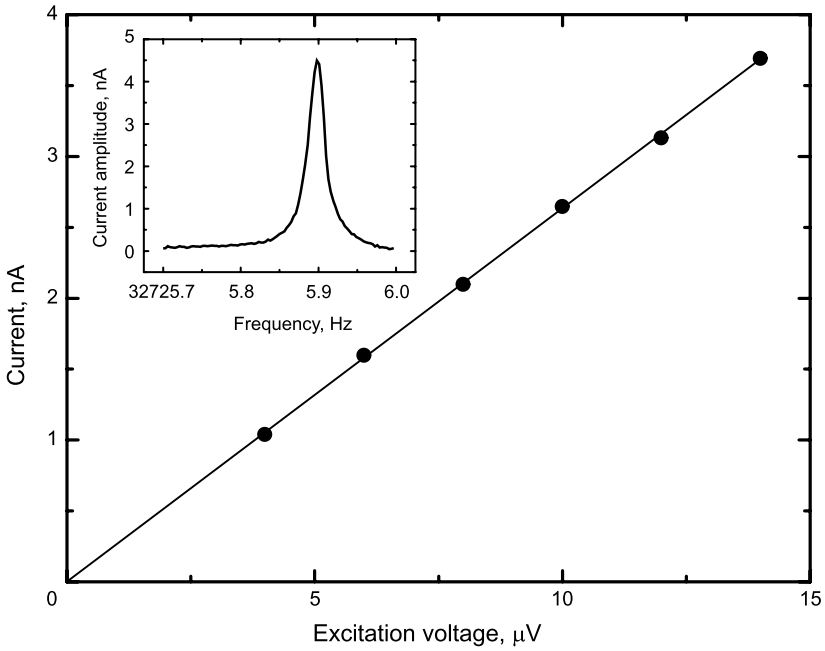

Fig. 2 The current–excitation voltage characteristic of the large tuning fork measured in vacuum at 0.9 K. The inset shows an example of its resonance characteristic with the width of the resonance ∼30 mHz

where m is the mass of the individual forks in vacuum, Δf_2^i is their intrinsic (vacuum) width of the resonance curve and R is the fork resistance. With the exception of the mass m, all other values were determined experimentally by measuring the amplitude-frequency characteristics of the fork at various excitations. As an example, the Fig. 2 shows the current–voltage dependence measured for the large fork. The slope of the characteristic determines the fork conductivity $(1/R)$. The inset to Fig. 2 shows the resonance characteristic of the large tuning fork as it was measured before the correction to the influence of the TTL (reference) output of the excitation generator on the measured current (for details we refer to [14]).

The mass of individual forks was determined as discussed in [2] i.e. for the mass m we take an effective mass of one prong of the fork in vacuum defined by $m = 0.24267\rho_q LWT$, where $\rho_q = 2659\ \mathrm{kg\,m^{-3}}$ is the density of quartz and L, W and T are the length, width and thickness of the quartz leg of individual forks, respectively. The three forks used in this work have dimensions: $L = 3.12$ mm, $W = 0.25$ mm and $T = 0.402$ mm giving $m = 2.0 \times 10^{-7}$ kg for the so called large fork, $L = 2.2$ mm, $W = 0.1$ mm and $T = 0.2$ mm giving $m = 2.84 \times 10^{-8}$ kg for so the called medium fork, and finally $L = 1.625$ mm, $W = 0.1$ mm and $T = 0.1$ mm giving $m = 1.05 \times 10^{-8}$ kg for the so called small fork. The α constants determined from measurements in vacuum for individual forks are as follow: $\alpha_L = 6.26 \times 10^{-6}$, $\alpha_M = 9.56 \times 10^{-7}$ and $\alpha_S = 1.04 \times 10^{-6}$ A.s.m^{-1}. It is worth stressing at this point that we think that the α_M constant was not determined properly due to an additional "transition" resistance, which accidentally appeared somewhere on the joints connecting the generator and

tuning fork and the I/V converter (a thermal contraction on the SMA connectors or silver conductive epoxy connecting the copper wires with the tuning fork). Due to this in series connected resistance with the tuning fork the voltage drop on the tuning fork is not the same as the excitation voltage, which leads to a distorted value of the α constant. Therefore, the physical characteristics measured using this medium fork are only qualitative.

3 Experimental Results

In general, the fork motion is damped by the liquid surrounding the fork. At temperatures below $0.25T_c$, the mean free path of excitations exponentially increases while the density of quasiparticles on the opposite, exponentially falls with decreasing temperature. As the tuning fork represents a macroscopic object, the fork motion in superfluid ^{3}He-B produces a backflow of nearby superfluid component around its prongs. Due to this superfluid flow, the ballistic excitations approaching the fork from a stationary superfluid "feel" a new frame of reference and their energy related to this frame of reference is shifted by $\Delta \pm \mathbf{p}_F.\mathbf{v}$. Here, $\mathbf{p}_F$ is the Fermi momentum, Δ is the energy gap and $\mathbf{v}$ is the velocity of the flow and characterizes the velocity field around the prong. The sign depends on the direction of the excitation motion with respect to the direction of the flow. Thus, the incoming excitations having the energy $\mathbf{p}_F.\mathbf{v} < \Delta$ will never reach the fork and they are reflected by the process of the Andreev reflection. This process is understood very well and in superfluid ^{3}He-B has been studied for the first time using a vibrating wire [15]. Following [15], the damping force per unit area acting on the fork motion can be, in general, expressed as

$$F_T = \kappa p_F \langle n v_g \rangle \left[1 - \exp\left(\frac{-\lambda p_F}{kT} v \right) \right], \tag{6}$$

where v_g is the group velocity of the excitations (quasiholes and quasiparticles), n is the number of excitations per unit volume, $\langle n v_g \rangle = n(p_F) kT \exp(-\Delta/kT)$ represents the quasiparticle flux with $n(p_F)$ being the density of states in the momentum space at the Fermi surface and κ and λ are the geometrical constants characterizing the fork geometry and velocity field profile, respectively.

Figure 3 shows the force – velocity dependencies (see (4) and (3)) measured at corresponding resonance frequencies for the large, medium and small tuning forks in superfluid ^{3}He-B at a temperature of 170 μK and pressure of 0.1 bar. While the dependence for the small fork clearly shows the "Andreev character" of the dependence i.e. a reduction of the damping force with increasing velocity, there is not such evidence in this dependence for the large and medium forks.

These measurements were performed using the full frequency sweeps for various excitation voltages in order to obtain complete physical information, namely the width of the resonance characteristic Δf_2 directly related to the damping processes expressed through the γ constant. In order to do that we use expression (6) and assuming that $p_F v \ll kT$, it is possible to expand the term $\exp(-\lambda p_F v/kT)$ in a Taylor

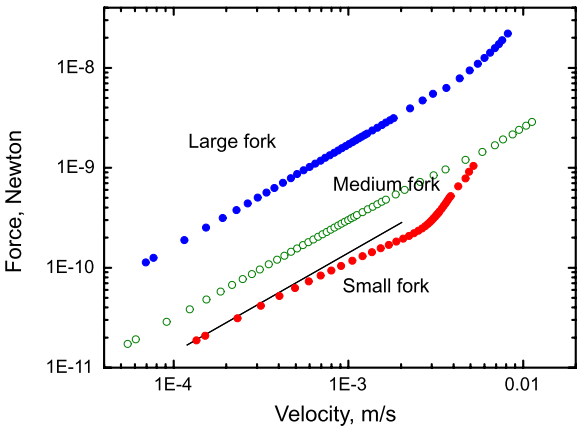

Fig. 3 (Color online) Force–velocity dependence as measured for the large, medium and small tuning forks in superfluid ^{3}He-B at a temperature of 170 μK and a pressure of 0.1 bar. The *line* is a guide for eyes

series. Taking into account the first three terms, one gets finally

$$F_T = \kappa n(p_F) p_F^2 \exp(-\Delta/kT)\lambda \left[1 - \frac{\lambda p_F}{2kT} v\right] \cdot v. \tag{7}$$

The total damping force can be parameterized as $F_T = \gamma_2 v = [\gamma_2(0) - \gamma_2(v)]v$. The first term in (7) describes the velocity independent damping coefficient $\gamma_2(0)$ and characterizes the region where the damping force depends linearly on the velocity ($F_T = \gamma_2(0)v$). The second term in (7) describes a contribution of the excitations being scattered by the Andreev process and as the fork velocity rises, the damping decreases as shown in Fig. 4 [9].

Figure 4 presents the dependencies of the damping constants $\gamma_2/2\pi$ i.e. the widths of the resonance characteristics Δf_2 as a function of the velocity for all three tuning forks. As one can see, there is a remarkable difference between the large fork and the others. The dependence of the small (and medium) tuning fork demonstrates the Andreev reflection process i.e. a linear decrease of the damping constant with the velocity increase (see (7) and we note the log. scale on the x axis), until a critical velocity is reached, when the fork begins to break the Cooper pairs. However, this dependence for the large tuning fork is opposite: the damping of the large fork increases with its velocity, until it reaches a maximum with a plateau. Then there is a small decrease of the damping constant on the further increase of the velocity probably due to Andreev reflection and finally, an expected rise of the damping when the pair breaking velocity is reached. Measurements presented in Fig. 4 were performed using full frequency sweeps with gradual increase of the excitation after each sweep for the fork being measured (e.g. large fork), while the second fork (e.g. small fork) simultaneously monitored temperature in the cell at constant resonant frequency and excitation. There was no additional heating observed until the pair-breaking velocity was reached.

At temperatures below 200 μK density of bulk excitations exponentially falls with temperature and normal component of superfluid ^{3}He practically vanishes. It is obvious that due to its larger mass, the large tuning fork is less sensitive to the scattering of the bulk excitations than the small (or medium) fork is. As one can see, the measured

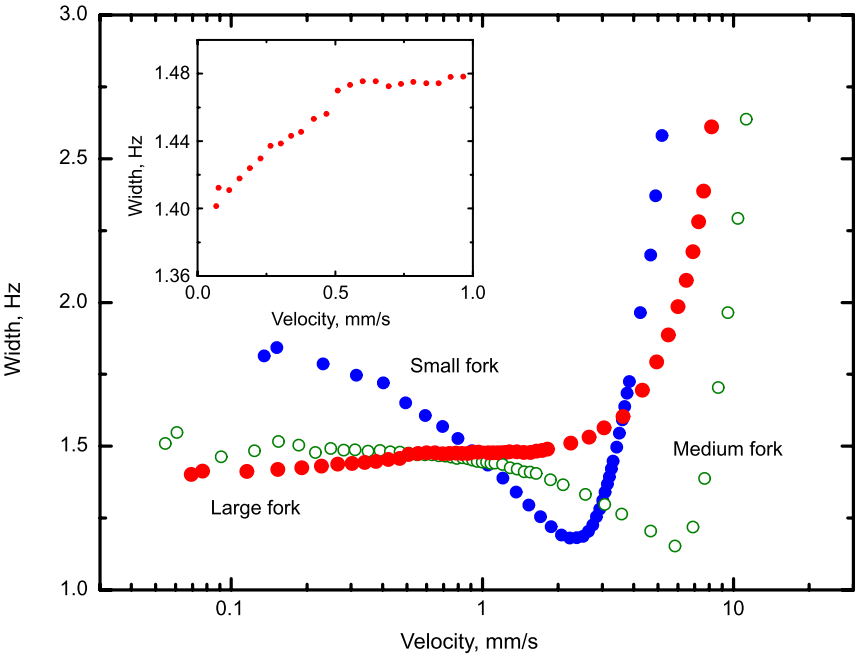

Fig. 4 (Color online) The dependence of the widths of the resonance characteristics as a function of the fork velocity measured for large, medium and small fork at temperature of 170 μK and a pressure of 0.1 bar. The *inset* shows the detail of this dependence for the large fork at low velocities (and corresponding small displacements)

width of the large fork showed in Fig. 4 is nearly two orders magnitude higher than the intrinsic width measured in vacuum ∼30 mHz. Also large fork's vacuum resonance frequency is about 500 Hz higher than that measured in superfluid ^{3}He-B at temperature 170 μK. The resonance frequency shift can be explained as a consequence of superfluid counterflow [16] when only hydrodynamic backflow term in expression for relative mass enhancement $\delta m/m$ is taken into account. In such case $\delta m/m = \rho_0/\rho_q$, where ρ_0 and ρ_q are densities of superfluid ^{3}He and quartz crystal, respectively. Using this fact, the relative frequency change $f_{0\mathrm{vac}}/f_0 = \sqrt{1+\delta m/m} \sim 1.5\%$ can be calculated, which corresponds to ∼500 Hz for the large fork.

The different width Δf_2 – velocity dependence for large fork presented in Fig. 4 suggests the presence of other dissipation mechanism than traditional Andreev reflection. Due to energy gap suppression near the fork surface there is a "space" created for excitations trapped in Andreev bound states. Quality of the fork surface (diffusive or specular) determine the density of states of these surface excitations [17]. We presume that at temperature 170 μK, the density of "Andreev excitations" trapped near the diffusive surface of large fork is larger than the density of volume excitations. When the large fork oscillates, it interacts with "Andreev excitations" and increases their energy. We assume that at low fork velocities, this energy enhancement is not enough for these excitations to escape from trapped state. They stay trapped but, having a higher energy, they cause higher damping of the fork motion. On the other hand,

the small (and medium) fork has smaller and much smoother surface than its large counterpart. Based on this picture, we presume that at sufficiently low temperatures, which will depend on area and quality of the surface, similar feature could be seen for medium and small fork as well. However to elucidate this mechanism more experimental work at the lowest temperatures is required. When the velocity is increased further and exceeds some critical value then the Cooper pairs start to break and this process manifests itself as a sudden increase of width (see Fig. 4). The critical velocity when the pair-breaking occurs is below the Landau velocity as a direct result of the existence of suppressed energy gap at the surface. This also implies the existence of bound states as was discussed in [18].

4 Conclusion

The main aim of our investigation was to compare the damping force acting on the high quality tuning forks with different sizes and geometries immersed in superfluid ^{3}He-B in the ballistic regime. The results presented confirm that the size of the fork determines its sensitivity with respect to the mutual interactions between the fork and ballistic excitations. While the properties of small (and medium) fork in superfluid ^{3}He-B seem to be equivalent to those of vibrating wires at temperature of 170 μK (e.g. presence of Andreev reflection), this is no longer valid in the case of large tuning fork because the width depends on velocity also in the region of small velocities. This implies the presence of some completely different dissipation mechanism, the physical origin of which is not yet properly understood. It may be caused by the interaction of the fork with the excitations trapped in the Andreev bound states. If it is so, this gives an opportunity to probe the Andreev bound states using tuning forks of different surface quality and it may lead to observation of new physical phenomena associated with these states as predicted in [19].

Acknowledgements Centre of Low temperature Physics is operated as the Center of Excellence of the APVV and the Slovak Academy of Sciences and P.J. Šafárik University under contracts VVCE-0058-07 and CE I-2/2007, respectively. This work is supported by the grants: APVV-0432-07, APVV-0346-07, VEGA 2/0025/09, EPSRC and by Microkelvin, the project of 7. FP of EU. Support provided by the U.S. Steel Košice s.r.o. is also very appreciated.

References

1. D.O. Clubb et al., J. Low Temp. Phys. **136**(1–2), 1 (2004)
2. R. Blaauwgeers et al., J. Low Temp. Phys. **146**(5–6), 537 (2007)
3. M. Blažková et al., J. Low Temp. Phys. **150**, 525 (2008)
4. A.P. Sebedash et al., J. Low Temp. Phys. **150**, 181 (2008)
5. E.M. Pentti et al., J. Low Temp. Phys. **150**, 555 (2008)
6. I.A. Gritsenko et al., J. Low Temp. Phys. **158**, 450 (2010)
7. M. Blažková et al., J. Low Temp. Phys. **148**, 305 (2007)
8. V.B. Efimov et al., J. Low Temp. Phys. **158**, 456 (2010)
9. D.I. Bradley, M. Človečko, E. Gažo, M. Kupka, P. Skyba, J. Low Temp. Phys. **152**, 147 (2008)
10. D.I. Bradley et al., J. Low Temp. Phys. **156**, 116 (2009)
11. D.I. Bradley et al., J. Low Temp. Phys. **157**, 476 (2009)

12. R.D. Grober, J. Acimovic, J. Schuck, D. Hessman, P.J. Kindlemann, J. Hespanha, S. Morse, K. Karrai, I. Tiemann, S. Manus, Rev. Sci. Instrum. **71**, 2776 (2000)
13. P. Skyba, J. Nyéki, E. Gažo, V. Makroczyová, Yu.M. Bunkov, D.A. Sergackov, A. Feher, Cryogenics **37**, 293 (1997)
14. P. Skyba, J. Low Temp. Phys. **160**(5–6), 219 (2010)
15. S.N. Fisher, A.M. Guénault, C.J. Kennedy, G.R. Pickett, Phys. Rev. Lett. **63**, 2566 (1989)
16. K. Penanen, R.E. Packard, Phys Rev. B **68**, 092504 (2003)
17. Y. Nagato, M. Yamamoto, K. Nagai, J. Low. Temp. Phys. **103**, 1135 (1998)
18. S.N. Fisher, A.M. Guénault, C.J. Kennedy, G.R. Pickett, Phys. Rev. Lett. **67**, 1270 (1991)
19. G.E. Volovik, JETP Lett. **91**, 201 (2010)